ORGANOMETALLICS

ARTICLE

pubs.acs.org/Organometallics

Synthesis, Structures, and Ethylene Dimerization Reactivity of Palladium Alkyl Complexes That Contain a Chelating Phosphine−Trifluoroborate Ligand

Youngmin Kim and Richard F. Jordan*

Department of Chemistry, The University of Chicago, 5735 South Ellis Avenue, Chicago, Illinois 60637, United States

Supporting Information

ABSTRACT: The chemistry of palladium alkyl complexes that incorporate the phosphine−trifluoroborate ligand *ortho*-$(Ph_2P)C_6H_4(BF_3^-)$ (PF^-) is described. The reaction of the pinacol borane *ortho*-$(Ph_2P)C_6H_4$(Bpin) with $K[HF_2]$ yields *ortho*-$(Ph_2P)C_6H_4(BF_3K)$ (K[PF], **1**). Crystallization of **1** from Et_2O/THF in the presence of 18-crown-6 yields [K-(18-crown-6)][PF]·0.5THF (**2**·0.5THF). In the solid state, the phosphine−borate anion of **2** is ion-paired with the [K-(18-crown-6)] cation through weak contacts with the phosphorus and two fluorine atoms. **1** reacts with (COD)PdMeCl in the presence of 18-crown-6 to form [K-(18-crown-6)][(PF)PdMeCl] (**3**) and with (COD)PdMeCl and 2,4,6-collidine (col) to yield (PF)PdMe(col) (**4**). The PF^- ligands in **3** and **4** are bound to Pd in a κ^2 mode through the phosphine and one fluorine of the $-ArBF_3^-$ unit. The other two fluorines are weakly bound to the $K(18\text{-crown-6})^+$ cation in **3**. NMR studies show that the Pd−F interactions in **3** and **4** are maintained in solution and that, for **4**, the three fluorine atoms undergo fast site exchange on the NMR time scale. **4** reacts with excess pyridine to yield (κ^1-*P*-PF)PdMe$(py)_2$ (**6**), in which the $-ArBF_3^-$ unit has been completely displaced by pyridine. **4** slowly dimerizes ethylene to 1-butene (36 t.o./h, 23 °C, CH_2Cl_2, 400 psi ethylene). The catalyst resting state is (PF)PdEt(col) (**7**). Addition of $[H(OEt_2)_2][B(3,5\text{-}(CF_3)_2\text{-}C_6H_3)_4]$ traps the collidine as [collidinium] $[B(3,5\text{-}(CF_3)_2\text{-}C_6H_3)_4]$ and results in a 10-fold increase in the ethylene dimerization rate (385 t.o./h, 23 °C, CD_2Cl_2, 150 psi ethylene).

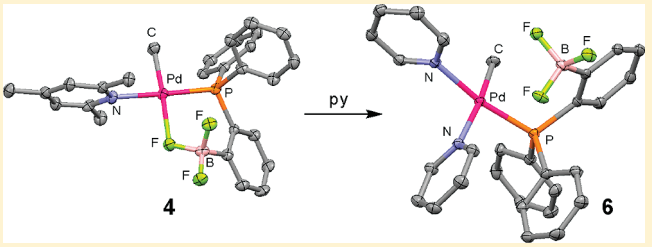

INTRODUCTION

Palladium(II) alkyl complexes (**A**) that contain *ortho*-phosphino-arenesulfonate ligands ($\{PO\}^-$) exhibit unique behavior in olefin polymerization. {PO}Pd(R)(L) (L = labile ligand) species polymerize ethylene to linear polyethylene and copolymerize ethylene with a variety of polar vinyl monomers to functionalized linear polymers.[1,2] $\{PO\}^-$ ligands contain two interesting features that may be related to the unusual behavior of {PO}Pd(R)(L) catalysts. First, the electronic asymmetry in {PO}Pd(R) species that results from the *cis* arrangement of the phosphine ligand, a strong donor, and the sulfonate ligand, a very weak donor, may inhibit β-H elimination and chain-walking processes that lead to the formation of branched polymers and disfavor β-X elimination processes that preclude ethylene/CH_2=CHX copolymerization by other catalysts. Second, the $\{PO\}^-$ ligand may potentially coordinate in a κ^3-*P,O,O* mode to facilitate *cis*/*trans* isomerization of {PO}Pd(R)(ethylene) species, which may be important for chain growth.[1j] The design of other ligands that feature these properties is of interest for developing new catalysts. Nozaki and Rieger have explored some aspects of the chemistry of Pd alkyl complexes that contain N-heterocyclic-carbene−sulfonate (**B**) and phosphine−phosphonate ligands (**C**).[3,4] Recently, Piers has observed hemilabile coordination behavior of the N-heterocyclic-carbene−trifluoroborate ligand in Rh complex **D**.[5] Here we describe the structures and reactivity of palladium alkyl complexes that incorporate the phosphine−trifluoroborate ligand *ortho*-$(Ph_2P)C_6H_4(BF_3^-)$.

RESULTS AND DISCUSSION

Synthesis and Structure of *ortho*-$(Ph_2P)C_6H_4(BF_3K)$ (K[PF], 1). The reaction of the pinacol borane *ortho*-$(Ph_2P)C_6H_4$(Bpin)[6] with $K[HF_2]$ in a mixture of MeOH and H_2O affords the phosphine−borate *ortho*-$(Ph_2P)C_6H_4(BF_3K)$ (K[PF], **1**) in 68% yield (Scheme 1). Compound **1** was characterized by multinuclear NMR spectroscopy and elemental analysis. The ^{31}P NMR spectrum comprises a quartet at δ −6.2 with J_{P-F} = 36 Hz. The ^{19}F (δ −135.2) and ^{11}B (δ 4.1) NMR chemical shifts of **1** are similar to those of the related phosphonium−borate zwitterion *ortho*-$(Ph_2MeP)C_6H_4(BF_3)$ (δ ^{19}F −139.0; δ ^{11}B 3.7).[7] Slow diffusion of Et_2O into a THF solution of **1** in the presence of 18-crown-6 results in crystallization of [K-(18-crown-6)][PF]·0.5THF (**2**·0.5THF), which was characterized by X-ray diffraction (Figure 1). The phosphine−borate anion of **2** is ion-paired with the [K-(18-crown-6)] cation through weak

Received: June 2, 2011
Published: July 19, 2011

Chart 1

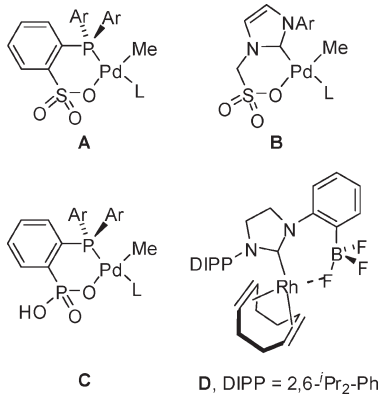

Scheme 1

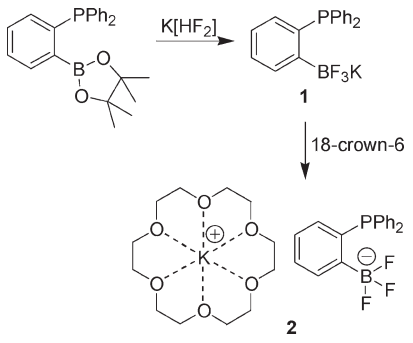

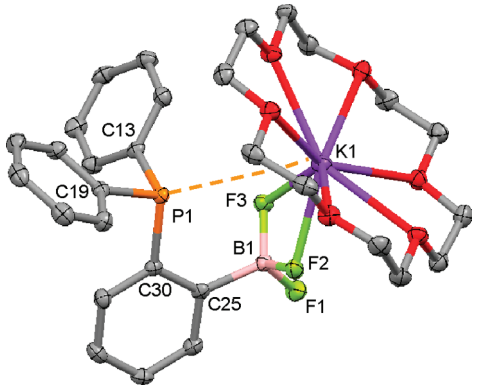

Figure 1. Molecular structure of [K-(18-crown-6)][PF] (**2**). Hydrogen atoms are omitted. Key bond lengths (Å) and angles (deg) not given in text: B(1)−F(1) 1.407(2), B(1)−F(3) 1.420(2), B(1)−F(2) 1.428(2), B(1)−C(25) 1.622(2), C(13)−P(1) 1.8361(17), C(19)−P(1) 1.8407(16), C(30)−P(1) 1.8392(17); F(1)−B(1)−F(3) 107.79(14), F(1)−B(1)−F(2) 107.21(14), F(3)−B(1)−F(2) 106.35(14), F(1)−B(1)−C(25) 110.79(14), F(3)−B(1)−C(25) 114.17(14), F(2)−B(1)−C(25) 110.21(13), C(13)−P(1)−C(30) 101.63(7), C(13)−P(1)−C(19) 100.77(7), C(30)−P(1)−C(19) 104.14(7).

contacts with the phosphorus and two fluorine atoms. The P1−K1 (3.8394(7) Å), F2−K1 (2.6435(11) Å), and F3−K1 (2.8021(11) Å) distances are all shorter than the corresponding sums of the van der Waals radii (P, K: 4.55 Å; F, K: 4.22 Å). The average of the B−F bond lengths in **2** (1.418 Å) is similar to that

Scheme 2

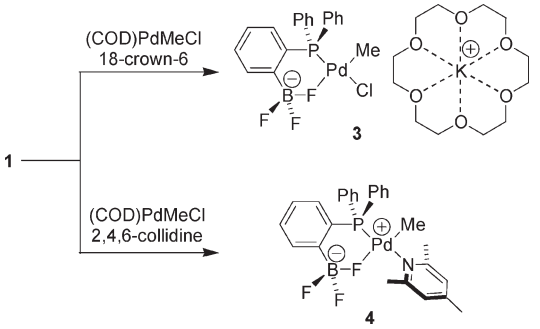

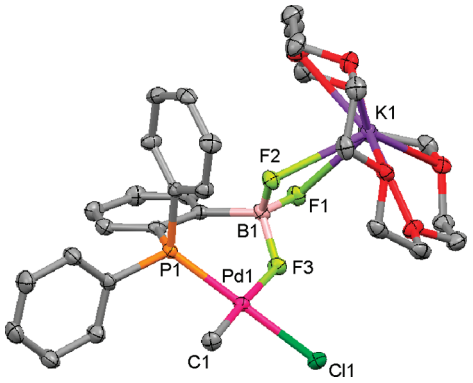

Figure 2. Molecular structure of [K-(18-crown-6)][(PF)PdMeCl] (**3**). Hydrogen atoms are omitted. Key bond lengths (Å) and angles (deg) not given in text: C(1)−Pd(1) 2.011(3), Cl(1)−Pd(1) 2.3569(8), P(1)−Pd(1) 2.2309(8); C(1)−Pd(1)−P(1) 90.29(9), F(3)−Pd(1)−P(1) 92.16(5), C(1)−Pd(1)−Cl(1) 90.89(9), F(3)−Pd(1)−Cl(1) 86.64(5).

for *ortho*-$(Ph_2MeP)C_6H_4(BF_3)$.[7] The F3−P1 distance in **2** (3.020 Å) is less than the corresponding sum of the van der Waals radii (F, P: 3.27 Å), and the F3−P1−C19 angle is nearly linear (177.9°), suggesting that a F(lone pair)→P(σ^*_{P-C}) interaction similar to that proposed for *ortho*-$(Ph_2MeP)C_6H_4(BF_3)$ is present.[7]

Synthesis and Structures of (PF)PdMeL Complexes. The reaction of **1** with (COD)PdMeCl in the presence of 18-crown-6 in THF affords [K-(18-crown-6)][(PF)PdMeCl] (**3**) in 67% yield (Scheme 2). The reaction of **1** with (COD)PdMeCl and 2,4,6-collidine (col) in CH_2Cl_2 affords (PF)PdMe(col) (**4**) in 64% yield.

The solid-state molecular structure of **3** is shown in Figure 2. The PF^- ligand binds to the square-planar Pd center in a κ^2 mode through the phosphine and one fluorine of the $ArBF_3^-$ unit. The K(18-crown-6)$^+$ cation binds the other two fluorines. The methyl group is *cis* to the phosphine. The six-membered (PF)Pd chelate ring is puckered, with an angle of 39.23° between the P−C−C−B and P−Pd−F planes. The Pd−F distance in **3** (Pd−F3 2.2144(16) Å) is similar to that in the η^1-BF_4^- complex (η^3-C_3H_5)Pd(NHC)(BF_4) (2.241(2) Å; NHC = C(N(^{t}Bu)CH)$_2$)[8] and much longer than the Pd−F distance in Pd^{II} terminal fluoride complexes (2.02−2.09 Å).[9] The Pd−F distance in **3** is intermediate between the sum of the Pd and F covalent (2.01 Å) and van der Waals (3.10 Å) radii. The PdF−B distance

dx.doi.org/10.1021/om200472x |*Organometallics* 2011, 30, 4250–4256

(F3−B1 1.446(4) Å) in **3** is ca. 0.04 Å longer than the other B−F distances (F1−B1 1.406(3), F2−B1 1.402(4) Å). The structure of **4** (Figure 3) is very similar to that of **3**. The (PF)Pd chelate ring in **4** is puckered, with an angle of 38.66° between the P−C−C−B and P−Pd−F planes, and the Pd−F, Pd−C, and Pd−P distances are essentially identical to the corresponding distances in **3**.

The $^{31}P\{^{1}H\}$ NMR spectra of **3** and **4** in CD_2Cl_2 solution at 23 °C consist of singlets at δ 30.2 and 29.0, respectively, which are shifted ca. 36 ppm downfield from the resonance of the free ligand **1**. The $^{19}F\{^{1}H\}$ spectra of **3** and **4** also comprise singlets (at δ −152.5 and −157.3, respectively) that are shifted upfield by ca. 20 ppm compared to the ^{19}F resonance of **1** (δ −135.2). The ^{19}F NMR resonances of **3** and **4** broaden but do not split when the temperature is lowered to −85 °C. The Pd−CH_3 ^{13}C NMR resonance of **3** appears as a broad singlet at 23 °C but sharpens to a doublet of doublets at −60 °C (δ −2.4, $J_{C-P} = J_{C-F} = 12$ Hz). The Pd−CH_3 ^{13}C NMR resonance of **4** at 23 °C appears as a quartet of doublets due to coupling to three fluorines and phosphorus (δ −2.9, $^{2}J_{C-F} = 12$ Hz, $^{2}J_{C-P} = 3$ Hz; Figure 4); cooling the solution to −80 °C results in broadening but no change in the multiplicity of this signal. These results show that the Pd−F interaction is maintained in solution under these conditions and that, for **4**, the three fluorine atoms undergo fast exchange on the NMR time scale.[10]

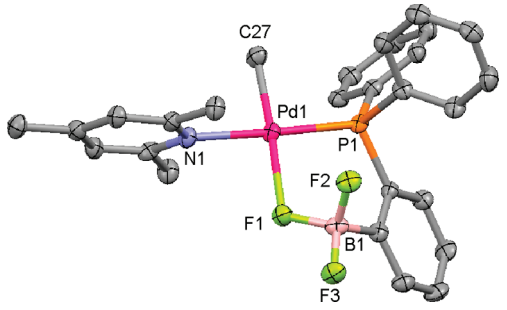

Figure 3. Molecular structure of (PF)PdMe(col) (**4**). Hydrogen atoms are omitted. Key bond lengths (Å) and angles (deg) not given in text: C(27)−Pd(1) 2.005(5), F(1)−Pd(1) 2.214(3), N(1)−Pd(1) 2.114(4), P(1)−Pd(1) 2.2338(14), B(1)−F(1) 1.467(7), B(1)−F(2) 1.397(6), B(1)−F(3) 1.378(7); C(27)−Pd(1)−N(1) 87.83(19), N-(1)−Pd(1)−F(1) 88.79(14), C(27)−Pd(1)−P(1) 89.87(16), F-(1)−Pd(1)−P(1) 93.52(9).

Reaction of 4 with Pyridine. The reaction of **4** with pyridine is summarized in Scheme 3. Addition of a small amount of pyridine (ca. 0.3 equiv) to a solution of **4** in CD_2Cl_2 at 23 °C generates an equilibrium mixture of **4** and the analogous pyridine complex **5** ($K_1 = [\mathbf{5}][\mathrm{col}]/[\mathbf{4}][\mathrm{py}] = 0.35(3)$) Exchange of **4** and **5** is slow on the NMR time scale, and separate resonances are observed for these species under these conditions. Addition of additional pyridine results in the expected shifting of the equilibrium toward **5** and the formation of the bis-ligand adducts (κ^1-*P*-PF)PdMe(py)$_2$ (**6**) and (κ^1-*P*-PF)PdMe(py)(col). The exchange of **6** with **5** is fast on the NMR time scale at 23 °C, and a single set of resonances at the weighted average chemical shifts of the these two species is observed. Similarly, one set of exchange-averaged resonances is observed for (κ^1-*P*-PF)PdMe(py)(col) and **4** under these conditions. The equilibrium constant for coordination of py to **5** to form **6** is $K_2 = [\mathbf{6}]/[\mathrm{py}][\mathbf{5}] = 45(5)$ M^{-1}. The addition of 35 equiv of pyridine to **4** results in complete conversion to **6**. The conversion of **4** to **5** or (κ^1-*P*-PF)PdMe(py)(col) and the conversion of **5** to **6** are presumed to occur by a standard associative substitution mechanism through five-coordinate intermediates ((κ^2-PF)PdMe(py)(col) and (κ^2-PF)PdMe(py)$_2$).

Complex **6** was isolated by crystallization by slow diffusion of Et_2O into a pyridine solution of **4**. The molecular structure of **6** is shown in Figure 5. Complex **6** features a square-planar geometry at Pd with a *cis* arrangement of the two pyridine ligands. The distance between the Pd and the nearest fluorine atom (F(3)) is 3.016 Å, which is close to the sum of the P and F van der Waals radii and indicates that the $-ArBF_3^-$ unit has been essentially completely displaced by pyridine. The $^{19}F\{^{1}H\}$ NMR spectrum of **6** in pyridine-d_5 comprises a singlet at δ −131.1, which falls in the same range as that for the free ligand **1** (δ = −135.2). Additionally, the Pd−CH_3 $^{13}C\{^{1}H\}$ NMR resonance of **6** appears as a doublet (δ 2.3, $J_{C-P} = 6$ Hz) with no detectable J_{C-F} coupling (Figure 4). These results are consistent with displacement of the $-ArBF_3^-$ by pyridine in solution as well as in the solid state. The structure of (κ^1-*P*-PF)PdMe(py)(col) is presumed to be analogous to that of **6**.

Dimerization of Ethylene by 4. Complex **4** slowly dimerizes ethylene to 1-butene, with a rate of ca. 36 t.o./h at 23 °C in CH_2Cl_2 solvent under 400 psi ethylene pressure. NMR analysis

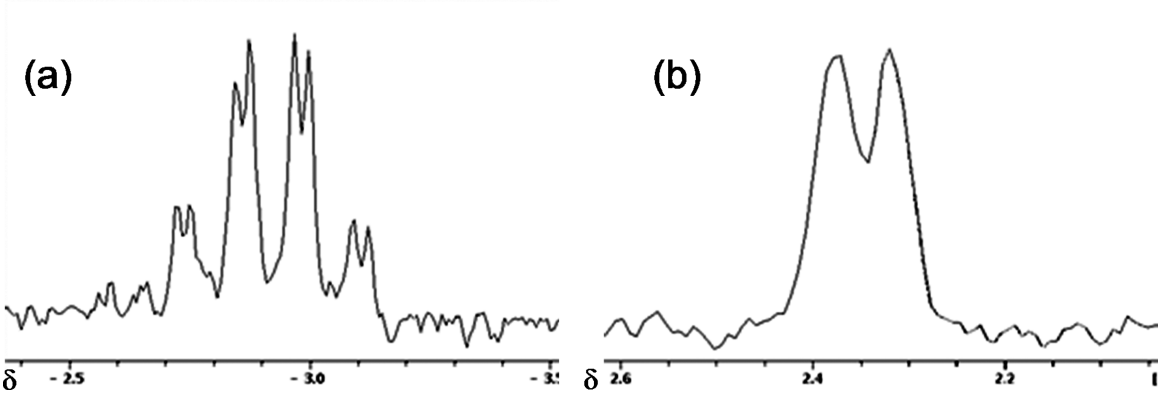

Figure 4. (a) Methyl region of the $^{13}C\{^{1}H\}$ NMR spectrum of (κ^2-PF)PdMe(col) (**4**) in CD_2Cl_2 at 23 °C showing J_{C-F} (12 Hz) and J_{C-P} (3 Hz) coupling, characteristic of fast exchange of Pd-coordinated and non-Pd-coordinated fluorines. (b) Methyl region of the $^{13}C\{^{1}H\}$ NMR spectrum of (κ^1-PF)PdMe(py)$_2$ (**6**) in pyridine-d_5 at 23 °C showing J_{C-P} (6 Hz) but not J_{C-F} coupling.

dx.doi.org/10.1021/om200472x |*Organometallics* 2011, 30, 4250–4256

Scheme 3

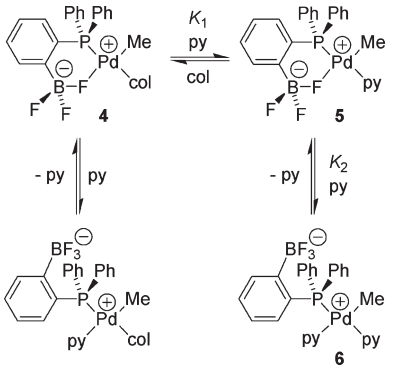

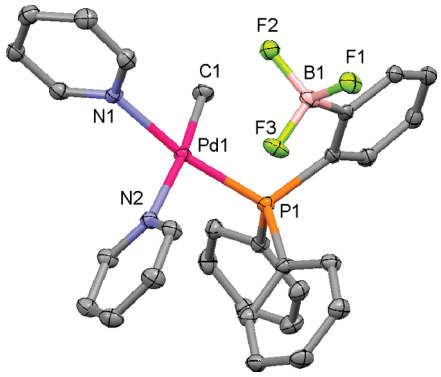

Figure 5. Molecular structure of (PF)PdMe(py)$_2$ (**6**). Hydrogen atoms are omitted. Key bond lengths (Å) and angles (deg): C(1)−Pd(1) 2.0523(17), N(1)−Pd(1) 2.1310(15), N(2)−Pd(1) 2.1647(14), P(1)−Pd(1) 2.2551(7); C(1)−Pd(1)−N(1) 86.95(6), N(1)−Pd(1)−N(2) 89.60(5), C(1)−Pd(1)−P(1) 87.81(5), N(2)−Pd(1)−P(1) 96.56(4).

of a CD_2Cl_2 solution of **4** under 150 psi ethylene after 3 h revealed the presence of propene, 1-butene, unreacted **4**, and a new Pd species, which has been characterized as the ethyl complex (PF)PdEt(col) (**7**). The $^{31}P\{^1H\}$ and $^{19}F\{^1H\}$ NMR spectra of **7** are very similar to those of the methyl analogue **4** and show that the PF^- ligand in **7** is coordinated in a κ^2-*P,F* fashion. The ^1H NMR spectrum of **7** contains singlets at δ 3.17 and 2.36 for the collidine Me groups, which are similar to the corresponding resonances of **4** and establish the presence of one collidine ligand. The Pd−Et resonances were assigned with the aid of COSY and $^1H\{^{19}F\}$ and $^1H\{^{31}P\}$ decoupling experiments (Figure 6). The Pd−CH_2CH_3 methylene resonance of **7** (δ 1.63) appears as a broadened doublet of quartets due to $^3J_{H-H}$ (7 Hz), $^3J_{H-P}$ (5 Hz), and small $^3J_{H-F}$ coupling. The Pd−CH_2CH_3 methyl resonance (δ 0.25) appears as a 12-line multiplet due to $^3J_{H-H}$ (7 Hz), $^4J_{H-P}$ (4 Hz), and $^4J_{H-F}$ (2 Hz) coupling. These spectroscopic features are similar to those observed for the related complex (*ortho*-$Ar_2PC_6H_4SO_3$)PdEt(2,6-lutidine) (Ar = *o*-$MeOC_6H_4$).[1j] These results are consistent with a dimerization mechanism involving displacement of collidine from resting state **7** by ethylene followed by insertion and chain transfer (Scheme 4).

Addition of 1 equiv of $[H(OEt_2)_2][B(3,5\text{-}(CF_3)_2\text{-}C_6H_3)_4]$[11] to trap the collidine as collidinium results in a ca. 10-fold increase in the rate of ethylene dimerization by **4**. At 23 °C in CD_2Cl_2 solvent and ca. 150 psi ethylene pressure, **4**/$[H(OEt_2)_2][B(3,5\text{-}(CF_3)_2\text{-}C_6H_3)_4]$ dimerizes ethylene with a rate of 385 t.o./h. Under these conditions, the primary product 1-butene is isomerized to *cis* and *trans* 2-butene.[12] NMR monitoring of the reaction of **4**, $[H(OEt_2)_2][B(3,5\text{-}(CF_3)_2\text{-}C_6H_3)_4]$, and ethylene shows that warming this mixture to −20 °C results in quantitative formation of [collidinium][$B(3,5\text{-}(CF_3)_2\text{-}C_6H_3)_4$] and a new Pd species characterized as (PF)PdMe(ethylene) (**8**).[13] At 0 °C, (PF)PdMe(ethylene) is converted to (PF)PdEt(ethylene) (**9**) with concomitant formation of propene and commencement of ethylene dimerization to 1-butene with **9** as the catalyst resting state. The NMR data for **8** and **9** are similar to the data for **4** and **7** except that the ^{31}P signals are shifted upfield by ca. 7 ppm, due to replacement of collidine by ethylene. Intermolecular exchange of bound ethylene with free ethylene is fast on the NMR time scale for these species, even at −80 °C.

CONCLUSION

The phosphine−borate ligand *ortho*-$(Ph_2P)C_6H_4(BF_3^-)$ binds to Pd(II) in a κ^2 mode through phosphorus and one fluorine to form [K(18-crown-6)][(κ^2-PF)PdMeCl] (**3**) and (κ^2-PF)PdMeL (L = collidine (**4**), pyridine (**5**)) complexes. In the presence of a large excess of pyridine, the $-ArBF_3^-$ unit of **4** is displaced and (κ^1-PF)PdMe$(py)_2$ (**6**) is formed. Complex **4** catalytically dimerizes ethylene to 1-butene by rate-limiting displacement of collidine by ethylene, insertion, and chain transfer. Trapping of the collidine by $[H(OEt_2)_2][B(3,5\text{-}(CF_3)_2\text{-}C_6H_3)_4]$ generates a base-free catalyst that is ca. 10 times more active for ethylene dimerization than **4**. Under these conditions, the catalyst resting state is (κ^2-PF)PdEt(ethylene).

EXPERIMENTAL SECTION

General Procedures. All experiments were performed using dry-box or Schlenk techniques under a nitrogen atmosphere. Nitrogen was purified by passage through activated molecular sieves and Q-5 oxygen scavenger. CH_2Cl_2 and CD_2Cl_2 were distilled from P_2O_5. MeOH was purchased from Aldrich (anhydrous, 99.8%). Hexanes, diethyl ether, and toluene were purified by passage through activated alumina and BASF R3-11 oxygen scavenger. 2-Isopropoxy-4,4,5,5-tetramethyl-1,3,2-dioxaborolane and $K[HF_2]$ were purchased from Aldrich. Ethylene (polymer grade) was purchased from Matheson Trigas and used as received. All other deuterated solvents were purchased from Cambridge Isotope Laboratories and used as received. NMR spectra of organometallic complexes were recorded on Bruker DMX-500 or DRX-400 spectrometers in Teflon-valved tubes at ambient temperature unless otherwise indicated. ^1H and ^{13}C chemical shifts are reported relative to $SiMe_4$ and were determined by reference to the residual ^1H and ^{13}C solvent resonances. ^{11}B, ^{19}F, and ^{31}P chemical shifts are referenced against external $BF_3\cdot Et_2O$, $CFCl_3$, and 85% H_3PO_4, respectively. For NMR assignments, C^1 is the carbon that is bonded to phosphorus.

X-ray Crystallography. Crystallographic details are provided in the Supporting Information. Data were collected on a Bruker Smart Apex diffractometer using Mo Kα radiation (0.71073 Å). Direct methods were used to locate many atoms from the E-map. Repeated difference Fourier maps allowed recognition of all expected non-hydrogen atoms. Following anisotropic refinement of all non-H atoms, ideal H-atom positions were calculated. Final refinement was anisotropic for all non-H atoms and isotropic-riding for H atoms. ORTEP diagrams are drawn with 50% probability ellipsoids.

Ethylene Dimerization. Ethylene dimerization reactions were performed in a 300 mL stainless steel Parr autoclave equipped with a

dx.doi.org/10.1021/om200472x |*Organometallics* 2011, 30, 4250–4256

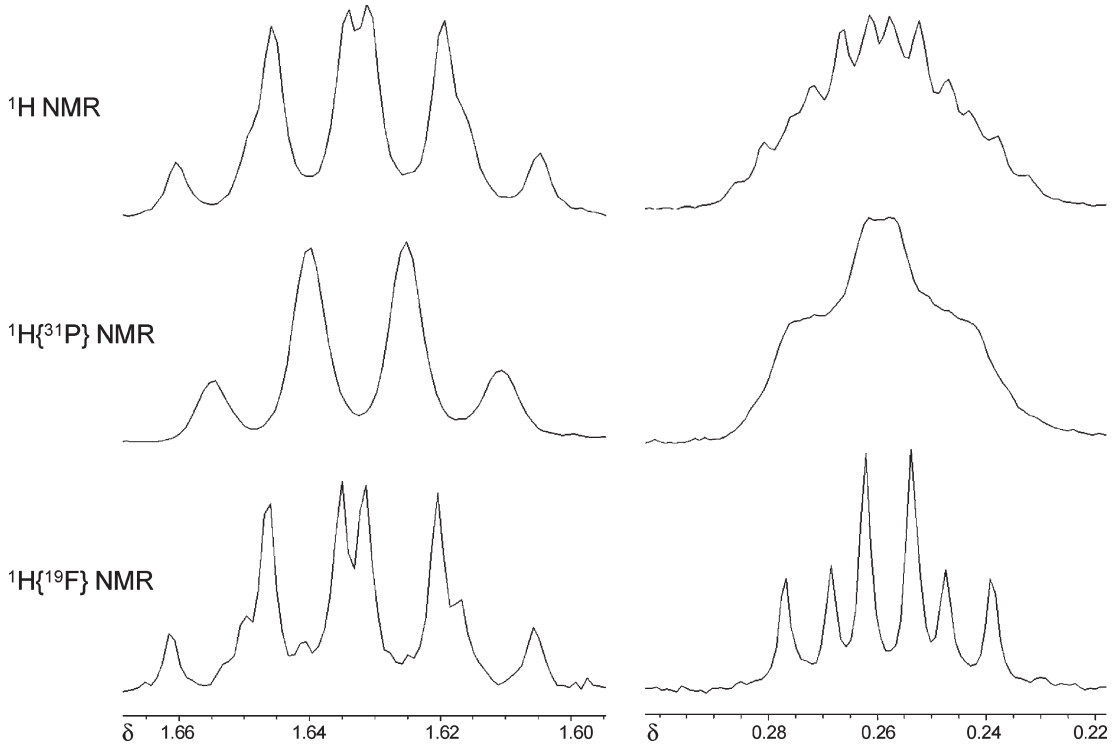

Figure 6. ^{1}H, ^{1}H{^{31}P}, and ^{1}H{^{19}F} NMR spectra of (PF)PdEt(col) (**7**) in CD_2Cl_2 at 23 °C. The PdCH_2CH$_3$ (left) and PdCH$_2$CH_3 (right) resonances are shown.

water cooling loop, thermocouple, and magnetically coupled stirrer and controlled by a Parr 4842 controller. In the glovebox, the catalyst solution or suspension was prepared in a glass liner. The liner was placed in the autoclave, and the autoclave was assembled and brought out of the box. The mixture was stirred at the rate of 200 rpm. The autoclave was pressurized with ethylene (400 psi). After 5 h, the mixture was cooled to −78 °C, the ethylene flow was terminated, and the pressure was released into a well-ventilated fume hood. The product was characterized by ^{1}H NMR spectroscopy. The yield of the product was measured using an internal standard by ^{1}H NMR spectroscopy.

***ortho*-(Ph$_2$P)C$_6$H$_4$(BF$_3$K) (1).** A solution of K[HF$_2$] (0.56 g, 7.2 mmol) in H$_2$O (5 mL) was added to a solution of *ortho*-(Ph$_2$P)C$_6$H$_4$-(Bpin)$_2$ (0.7 g, 1.8 mmol) in MeOH (15 mL). The mixture was stirred at 23 °C for 1 h. A white precipitate formed. The mixture was filtered to afford a white solid. The solid was washed sequentially with H$_2$O, Et$_2$O, a mixture of MeOH/Et$_2$O (1/6, v/v), and CH$_2$Cl$_2$ and then dried under the vacuum to afford a white solid. Yield: 0.45 g (68%). ^{1}H NMR (acetone-d_6): δ 7.73 (br s, 1H, H^3-Ar), 7.23 (m, 10H, *H*-Ph), 7.13 (t, $J_{H-H} = J_{H-P} = 7$, 1H, H^6-Ar), 7.00 (t, $J_{H-H} = 7$, 1H, H^4-Ar), 6.91 (m, 1H, H^5-Ar). ^{13}C{^{1}H} NMR (acetone-d_6): δ 141.6 (d, $J_{C-P} = 14$), 139.4 (d, $J_{C-P} = 13$), 134.2 (d, $J_{C-P} = 19$, C^2-Ph), 133.4 (dq, $J_{C-P} = 14$, $J_{C-F} =$ 3 Hz, C^3-Ar), 128.7 (d, $J_{C-P} = 7$, C^3-Ph), 128.3 (C^4-Ph), 127.8 (C^6-Ar), 126.6 (C^4-Ar). (The C^5-Ar peaks overlap with the C^2-Ph peaks, and the C^2-Ar resonance was not observed.) ^{11}B{^{1}H} NMR (acetone-d_6) δ 4.1 (br s). ^{31}P{^{1}H} NMR (acetone-d_6): δ −6.2 (q, $J_{P-F} = 36$). ^{19}F{^{1}H} NMR (acetone-d_6): δ −135.2 (br s). Anal. Calcd for $C_{18}H_{14}BF_3KP$: C, 58.72; H, 3.83. Found: C, 58.87; H, 3.93.

[K-(18-crown-6)][PF] (2). Slow diffusion of Et$_2$O into a THF solution of **1** in the presence of 18-crown-6 yields crystals of **2**. **2** was characterized by X-ray diffraction.

[K-(18-crown-6)][(PF)PdMeCl] (3). A flask was charged with (COD)PdMeCl (0.073 g, 0.27 mmol), **1** (0.10 g, 0.27 mmol), and 18-crown-6 (0.088 g, 0.33 mmol). THF (5 mL) was added, and the mixture was stirred at 23 °C for 1 h. A pale yellow precipitate formed. The

Scheme 4

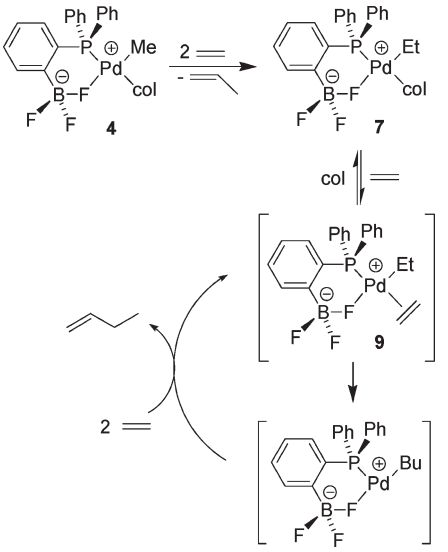

volatiles were removed under vacuum. The residue was washed with Et$_2$O followed by THF to yield a white solid. Yield: 0.15 g (67%). ^{1}H NMR (CD_2Cl_2): δ 7.75 (m, 1H, H^3-Ar), 7.53 (m, 4H, H^2-Ph), 7.42 (m, 6H, H^3-Ph and H^4-Ph), 7.34 (t, 1H, $J_{H-H} = J_{H-P} = 7$, H^6-Ar), 7.14 (t, 1H, $J_{H-H} = 7$, H^4-Ar), 6.88 (t, 1H, $J_{H-H} = 8.8$, H^5-Ar), 3.57 (s, 24H, O(CH_2)$_2$O), 0.76 (br s, 3H, PdCH_3). ^{13}C{^{1}H} NMR (CD_2Cl_2): δ 134.7 (d, $J_{C-P} = 12$, C^2-Ph), 133.3 (d, $J_{C-P} = 4$, C^3-Ar), 132.73, 133.2 (C^5-Ar), 132.7 (d, $J_{C-P} = 50$), 130.4 (d, $J_{C-P} = 2$, C^4-Ph), 129.6 (C^6-Ar), 128.6 (d, $J_{C-P} = 11$, C^3-Ph), 126.9 (d, $J_{C-P} = 7$, C^4-Ar), 70.4 (s, O(CH_2)$_2$O), −2.4 (br s, PdCH_3) (C^2-Ar resonance was not observed). ^{11}B{^{1}H} NMR (CD_2Cl_2): δ 2.5 (br s). ^{31}P{^{1}H} NMR (CD_2Cl_2): δ

dx.doi.org/10.1021/om200472x |*Organometallics* 2011, 30, 4250–4256

30.2. $^{19}F\{^1H\}$ NMR (CD_2Cl_2): δ −152.5 (br s). Anal. Calcd for $C_{33}H_{45}BClF_3KO_{6.5}PPd$(0.5THF): C, 48.02; H, 5.49. Found: C, 48.68; H, 5.70.

(PF)PdMe(col) (4). A flask was charged with (COD)PdMeCl (0.10 g, 0.38 mmol) and **1** (0.14 g, 0.38 mmol). A solution of 2,4,6-collidine (0.060 mL, 0.45 mmol) in CH_2Cl_2 (5 mL) was added, and the mixture was stirred at 23 °C for 1 h to form a solution. The solution was filtered, and the filtrate was taken to dryness under vacuum. The residue was dissolved in benzene and filtered, and the filtrate was concentrated to afford a pale yellow precipitate, which was collected and dried under vacuum. The solid was recrystallized from CH_2Cl_2/Et_2O to yield a white solid. Yield: 0.14 g (64%). ^1H NMR (CD_2Cl_2): δ 7.76 (dd, J_{H-H} = 7, J_{H-P} = 3, 1H, H^3-Ar), 7.58 (m, 4H, H^2-Ph), 7.49 (m, 6H, H^3-Ph and H^4-Ph), 7.39 (t, J_{H-H} = J_{H-P} = 7 Hz, 1H, H^6-Ar), 7.20 (t, J_{H-H} = 7, 1H, H^4-Ar), 7.06 (s, 2H, col), 6.95 (m, 1H, H^5-Ar), 3.10 (s, 3H, *o*-col-CH_3), 2.35 (s, 3H, *p*-col-CH_3), 0.53 (d, J_{H-P} = 2, 3H, $PdCH_3$). $^{13}C\{^1H\}$ NMR (CD_2Cl_2): δ 158.6 ($C^{2,6}$-col), 151.4 (C^4-col), 134.4 (d, J_{C-P} = 11, C^2-Ph), 133.4 (m, C^3-Ar), 133.2 (m, C^5-Ar), 131.7 (d, J_{C-P} = 47), 131.5 (d, J_{C-P} = 52), 130.9 (d, J_{C-P} = 3, C^4-Ph), 130.2 (C^6-Ar), 128.9 (d, J_{C-P} = 11, C^3-Ph), 127.3 (d, J_{C-P} = 8, C^4-Ar), 124.1 (d, J_{C-P} = 3, C^3-col), 26.2 (*o*-col-CH_3), 21.0 (*p*-col-CH_3), −2.9 (qd, J_{C-F} = 12, J_{C-P} = 3, $PdCH_3$) (C^2-Ar resonance was not observed). $^{11}B\{^1H\}$ NMR (CD_2Cl_2): δ 2.6 (br s). $^{31}P\{^1H\}$ NMR (CD_2Cl_2): δ 29.0. $^{19}F\{^1H\}$ NMR (CD_2Cl_2): δ −157.3 (br s). Anal. Calcd for $C_{27}H_{28}BF_3NPPd$: C, 56.72; H, 4.94. Found: C, 56.48; H, 5.09.

(PF)PdMe(py)$_2$ (6). Single crystals of **6** were obtained by slow diffusion of Et_2O into a solution of **4** in pyridine at 23 °C. Due to the rapid equilibrium between **5** and **6**, NMR analysis of **6** performed in pyridine-d_5 solution and therefore signals for coordinated pyridine were not observed. ^1H NMR (pyridine-d_5): δ 8.87 (m, 1H, H^3-Ar), 7.69 (br s, 4H, H^2-Ph), 7.57 (m, 1H, *H*-Ar), 7.31 (m, 2H, H^4-Ph), 7.29 (m, 1H, *H*-Ar), 7.20 (br s, 1H, *H*-Ar), 7.16 (br s, 4H, H^3-Ph), 0.91(d, J_{H-P} = 3, 3H, $PdCH_3$). $^{13}C\{^1H\}$ NMR (pyridine-d_5): δ 136.6 (m, C^3-Ar), 134.9 (d, J_{C-P} = 48), 132.1 (d, J = 7, *C*-Ar), 131.5 (d, J_{C-P} = 54), 130.0 (C^4-Ph), 130.0 (*C*-Ar), 128.5 (d, J_{C-P} = 10, C^3-Ph), 126.4 (d, J_{C-P} = 9, *C*-Ar), 2.3 (d, J_{C-P} = 6, $PdCH_3$); the C^2-Ph peaks overlap with the solvent peaks and C^2-Ar resonance was not observed. $^{31}P\{^1H\}$ NMR (pyridine-d_5): δ 42.9 (q, J_{P-F} = 11). $^{19}F\{^1H\}$ NMR (pyridine-d_5): δ −131.1 (br s). $^{11}B\{^1H\}$ NMR (pyridine-d_5): δ 4.4 (br s).

(PF)Pd(Et)(col) (7). ^1H NMR (CD_2Cl_2): δ 7.75 (dd, J_{H-H} = 7, J_{H-P} = 3, 1H, H^3-Ar), 7.63 (m, 4H, H^2-Ph), 7.50 (m, 6H, H^3-Ph and H^4-Ph), 7.40 (m, 1H, *H*-Ar), 7.21 (m, 1H, *H*-Ar), 7.07 (s, 2H, col), 7.06 (m, 1H, *H*-Ar), 3.17 (s, 6H, *o*-col-Me), 2.36 (s, 3H, *p*-col-Me), 1.63 (qd, J_{H-H} = 7, J_{H-P} = 5, 2H, Pd-CH_2CH_3), 0.25 (m, J_{H-H} = 7, J_{H-P} = 4, J_{H-F} = 2, 3H, Pd-CH_2CH_3). $^{31}P\{^1H\}$ NMR (CD_2Cl_2): δ 29.2. $^{19}F\{^1H\}$ NMR (CD_2Cl_2): δ −155.7 (br s).

(PF)PdMe(ethylene) (8). ^1H NMR (CD_2Cl_2, −40 °C, in presence of 2.2 equiv of free ethylene): δ 7.48 (m, 2H, *H*-Ph), 7.41 (m, 9H, *H*-Ph and *H*-Ar), 7.25 (t, J_{HH} = 7, 1H, *H*-Ar), 6.93 (m, 1H, *H*-Ar), 5.43 (coordinated and free ethylene), 0.70 (s, 3H, Pd-CH_3); the H^3-Ar resonances overlap with the $[B(3,5\text{-}(CF_3)_2\text{-}C_6H_3)_4]^-$ signals. $^{13}C\{^1H\}$ NMR (CD_2Cl_2, −40 °C, in presence of 2.2 equiv of free ethylene): δ 133.9 (d, J_{C-P} = 12, C^2-Ph), 133.3 (C-Ar), 132.6 (m, C-Ar), 131.1 (C^4-Ph), 130.3 (*C*-Ar), 129.8 (d, J_{C-P} = 49), 129.0, 128.7 (d, J_{C-P} = 11, C^3-Ph), 127.8 (d, J_{C-P} = 7, *C*-Ar), 119 (br s, coordinated and free ethylene; this resonance correlates with the ^1H NMR ethylene resonance in the HMQC spectrum), 4.5 (m, $PdCH_3$); the C^2-Ar resonance was not observed. $^{31}P\{^1H\}$ NMR (CD_2Cl_2, −20 °C): δ 22.2. $^{19}F\{^1H\}$ NMR (CD_2Cl_2, −20 °C): δ −151.5 (br s).

(PF)Pd(Et)(ethylene) (9). ^1H NMR (CD_2Cl_2, 0 °C, in the presence of 66 equiv of free ethylene): δ 7.48 (m, 11H, *H*-Ph and *H*-Ar), 7.29 (t, J_{HH} = 7, 1H, *H*-Ar), 7.19 (m, 1H, *H*-Ar), 1.83 (p, J_{H-H} = 7, J_{H-P} = 7, 2H, $PdCH_2CH_3$), 0.42 (m, 3H, $PdCH_2CH_3$); the H^3-Ar resonances overlap with the $[B(3,5\text{-}(CF_3)_2\text{-}C_6H_3)_4]^-$ signals; the ethylene signal was not observed due to fast intermolecular ethylene exchange. $^{31}P\{^1H\}$ NMR (CD_2Cl_2, 0 °C): δ 22.5. $^{19}F\{^1H\}$ NMR (CD_2Cl_2, 0 °C): δ −149.7 (br s).

(PF)Pd(Me)(OEt$_2$). ^1H NMR (CD_2Cl_2, −60 °C): δ 7.69 (m, 1H, H^3-Ar), 7.44 (m, 11H, *H*-Ph and *H*-Ar), 7.21 (m, 1H, *H*-Ar), 6.84 (m, 1H, *H*-Ar), 3.74 (q, J_{HH} = 7, 4H, OCH_2CH_3), 1.71 (t, 6H, J_{HH} = 7, OCH_2CH_3), 0.58 (s, 3H, $PdCH_3$). $^{31}P\{^1H\}$ NMR (CD_2Cl_2, −60 °C): δ 34.8. $^{19}F\{^1H\}$ NMR (CD_2Cl_2, −60 °C): δ −152.4 (br s). $^{13}C\{^1H\}$ NMR (CD_2Cl_2, −40 °C): δ 133.6 (d, J_{C-P} = 12, C^2-Ph), 132.9 (d, J_{C-P} = 6, *C*-Ar), 132.7 (m, *C*-Ar), 130.88 (d, J_{C-P} = 2, C^4-Ph), 130.7, 130.3 (*C*-Ar), 129.5 (d, J_{C-P} = 58), 128.6 (d, J_{C-P} = 11, C^3-Ph), 127.5 (C-Ar), 70.2 (br s, $Pd(OCH_2CH_3)_2$), 16.3 (br s, $Pd(OCH_2CH_3)_2$), 2.7 (br s, $PdCH_3$); the C^2-Ar resonance was not observed.

■ ASSOCIATED CONTENT

Supporting Information. Representative NMR spectra and crystallographic data (CIF files). This material is available free of charge via the Internet at http://pubs.acs.org.

■ AUTHOR INFORMATION

Corresponding Author
*E-mail: rfjordan@uchicago.edu.

■ ACKNOWLEDGMENT

This work was supported by the National Science Foundation (CHE-0911180).

■ REFERENCES

(1) (a) Drent, E.; Dijk, R.; Ginkel, R.; Oort, B.; Pugh, R. I. *Chem. Commun.* **2002**, 744.(b) Drent, E.; Pello, D. H. L. Eur. Pat. 0632084, 1995. (c) Kochi, T.; Yoshimura, K.; Nozaki, K. *Dalton Trans.* **2006**, 25. (d) Vela, J.; Lief, G. R.; Shen, Z.; Jordan, R. F. *Organometallics* **2007**, *26*, 6624. (e) Skupov, K. M.; Marella, P. R.; Simard, M.; Yap, G. P. A.; Allen, N.; Conner, D.; Goodall, B. L.; Claverie, J. P. *Macromol. Rapid Commun.* **2007**, *28*, 2033. (f) Kochi, T.; Noda, S.; Yoshimura, K.; Nozaki, K. *J. Am. Chem. Soc.* **2007**, *129*, 8948. (g) Luo, S.; Vela, J.; Lief, G. R.; Jordan, R. F. *J. Am. Chem. Soc.* **2007**, *129*, 8946. (h) Weng, W.; Sheng, Z.; Jordan, R. F. *J. Am. Chem. Soc.* **2007**, *129*, 15450. (i) Guironnet, D.; Roesle, P.; Rünzi, T.; Götter-Schnetmann, I.; Mecking, S. *J. Am. Chem. Soc.* **2009**, *131*, 422. (j) Noda, S.; Nakamura, A.; Kochi, T.; Chung, L. W.; Morokuma, K.; Nozaki, K. *J. Am. Chem. Soc.* **2009**, *131*, 14088. (k) Ito, S.; Munakata, K.; Nakamura, A.; Nozaki, K. *J. Am. Chem. Soc.* **2009**, *131*, 14606. (l) Rünzi, T.; Fröehlich, D.; Mecking, S. *J. Am. Chem. Soc.* **2010**, *132*, 17690. (m) Drent, E.; van Dijk, R.; van Ginkel, R.; van Oort, B.; Pugh, R. I. *Chem. Commun.* **2002**, 964. (n) Hearley, A. K.; Nowack, R. J.; Rieger, B. *Organometallics* **2005**, *24*, 2755. (o) Bettucci, L.; Bianchini, C.; Claver, C.; Suarez Eduardo, J. G.; Ruiz, A.; Meli, A.; Oberhauser, W. *Dalton Trans.* **2007**, 5590. (p) Newsham, D. K.; Borkar, S.; Sen, A.; Conner, D. M.; Goodall, B. L. *Organometallics* **2007**, *26*, 3636. (q) Nozaki, K.; Kusumoto, S.; Noda, S.; Kochi, T.; Chung, L. W.; Morokuma, K. *J. Am. Chem. Soc.* **2010**, *132*, 16030.

(2) For reviews, see: (a) Nakamura, A.; Ito, S.; Nozaki, K. *Chem. Rev.* **2009**, *109*, 5215. (b) Andreas, B.; Mecking, S. *Angew. Chem., Int. Ed.* **2008**, *47*, 2538.

(3) Nagai, Y.; Kochi, T.; Nozaki, K. *Organometallics* **2009**, *28*, 6131.

(4) Reisinger, C. M.; Nowack, R. J.; Volkmer, D.; Rieger, B. *Dalton Trans.* **2007**, 272.

(5) Gott, A. L.; Piers, W. E.; McDonald, R.; Parvez, M. *Inorg. Chim. Acta* **2011**, *369*, 180.

(6) Porcel, S.; Bouhadir, G.; Saffon, N.; Maron, L.; Bourissou, D. *Angew. Chem., Int. Ed.* **2010**, *49*, 6186.

(7) Wade, C. R.; Zhao, H.; Gabbai, F. P. *Chem. Commun.* **2010**, *46*, 6380.
(8) Chernyshova, E. S.; Goddard, R.; Poerschke, K.-R. *Organometallics* **2007**, *26*, 3236.
(9) (a) Grushin, V. V.; Marshall, W. J. *Angew. Chem., Int. Ed.* **2002**, *41*, 4476. (b) Yahav, A.; Goldberg, I.; Vigalok, A. *J. Am. Chem. Soc.* **2003**, *125*, 13634. (c) Jasim, N. A.; Perutz, R. N.; Whitwood, A. C.; Braun, T.; Izundu, J.; Neumann, B.; Rothfeld, S.; Stammler, H.-G. *Organometallics* **2004**, *23*, 6140.
(10) Mechanisms for the exchange of terminal and bridging fluorines that involve (κ^1-*P*-PF)Pd and (κ^3-*P,F,F*-PF)Pd intermediates or transition states are possible. For a detailed analysis of the dynamic properties of tungsten BF_4^- complexes see: Honeychuck, R. V.; Hersh, W. H. *J. Am. Chem. Soc.* **1989**, *111*, 6056.
(11) Brookhart, M.; Grant, B; Volpe, A. F. *Organometallics* **1992**, *11*, 3920.
(12) Control experiments show that [collidinium] [B(3,5-$(CF_3)_2$-$C_6H_3)_4$] does not isomerize α-olefins under these conditions. Isomerization likely occurs by formation and chain walking of Pd-Bu species.
(13) The reaction of **4** with 1 equiv of [$H(OEt_2)_2$][B(3,5-$(CF_3)_2$-$C_6H_3)_4$] in CD_2Cl_2 at −60 °C followed by warming to −20 °C in the absence of ethylene yields (PF)PdMe(OEt_2).